

Biological Bottom-Up Assembly of Antibody Nanotubes on Patterned Antigen Arrays

Nurxat Nuraje, Ipsita A. Banerjee, Robert I. MacCuspie, Lingtao Yu, and Hiroshi Matsui*

*Department of Chemistry and Biochemistry at Hunter College and the Graduate Center,
The City University of New York, New York, New York 10021*

Received March 10, 2004; E-mail: hmatsui@hunter.cuny.edu

The bottom-up approach in nanofabrication has been studied extensively due to the potential to develop devices such as electronics, actuators, and sensors more efficiently and economically compared to existing technologies.¹ Application of biotechnology in nanofabrication also has an advantage to produce functional building-block materials that may not have synthetic counterparts in much milder experimental conditions, such as room temperature and ambient pressure.² Various building blocks have been developed for the biological bottom-up approach;³ however, it is necessary for these building blocks to be addressed to the exact locations with high precision and reproducibility to function in the nanometer-scale devices.^{1a,4,5} Recently, carbon nanotubes were assembled on regions coated with the polar chemical groups on large scale.⁶

Here we introduced a new type of building block, antibody nanotubes, and demonstrated anchoring them on complementary antigen arrays via antibody–antigen recognition. Biological recognition between the antibody nanotubes and the antigen arrays permitted recognition-driven assembly of ordered nanotube arrays. The array of antigens was written by using the tip of an atomic force microscope (AFM) on alkylthiol self-assembled monolayer (SAM)-coated Au substrates via nanografting.⁷ After antigens were immobilized onto the shaved regions of the alkylthiol SAMs with the AFM tip, antibody nanotubes, produced by incubating antibodies in template nanotube solutions, were selectively attached onto the antigen regions (Figure 1).

A template nanotube self-assembled from bolaamphiphile peptide monomers in NaOH/citric acid solution via three-dimensional intermolecular hydrogen bonds^{8,9} has been demonstrated to immobilize various proteins and peptides on nanotube surfaces.¹⁰ This template nanotube immobilizes proteins and peptides at free amide sites on the nanotube sidewall via hydrogen bonding by means of simple incubations, the detailed procedures of which were published previously.^{10b,11} After those nanotubes were centrifuged and run through size-separation columns, a 1-mL solution of the resulting nanotubes (10 mM) with an average diameter of 100 nm were incubated with a 1-mL solution of goat anti-mouse IgG in a pH 7.2 phosphate buffer (50 $\mu\text{g}/\text{mL}$). After 48 h, the anti-mouse IgG was coated on the template nanotubes to form the antibody nanotubes. The anti-mouse IgG nanotubes were washed with Nanopure water and centrifuged twice to remove unbound anti-mouse IgG before mixing with the antigen-coated substrates. The attachment of anti-mouse IgG on the nanotube was confirmed by fluorescence microscopy. The FITC-labeled anti-mouse IgG on the nanotube was also confirmed to recognize and bind the mouse IgG in solution. These results are shown in Supporting Information.

To observe the selective immobilization of antibody nanotubes on the mouse-IgG arrays, systematic AFM analyses for the resulting substrates were applied (Figure 2). After 1-octadecanethiol (0.01 mM) was self-assembled on Au substrates in 99% ethanol at room

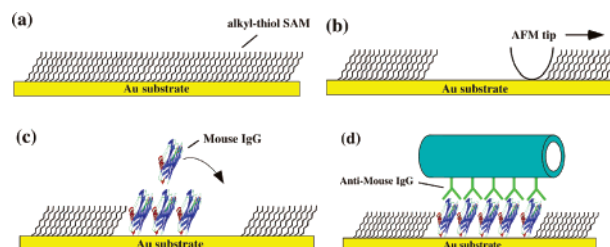


Figure 1. Schematic diagram of the antibody nanotube assembly on the complementary antigen substrates via biological recognition. (a) Self-assembly of alkylthiol monolayers on Au substrates. (b) Shaving trenches on the alkylthiol SAM by using the AFM tip (nanoshaving). (c) Deposition of antigens in the shaved trenches (nanografting). (d) Location-specific immobilization of the antibody nanotube onto the complementary antigen regions via the biological recognition.

temperature for 24 h (Figure 2a), a series of trenches (400 nm \times 4 μm) were made by shaving the alkylthiol SAM with a Si_3N_4 tip (Veeco Metrology) of the AFM (Nanoscope IIIa and MultiMode microscope, Digital Instruments), as shown in Figure 2b (left). These trenches were patterned by using a customized Nanoscript software (Veeco Metrology). The section analysis of the trenches in Figure 2b (right) shows that the depth of all trenches (marked by black dotted lines) is 10 nm. The substrate was washed sequentially first with ethanol and then with hexane, but the alkylthiol molecules removed by the AFM tip were still partially piled up and remained at the edges of trenches as shown in Figure 2b (left). After the mouse IgG was incubated with the resulting substrates for 1 h at room temperature, the mouse IgG was deposited on the trenches via the thiol–Au interaction (Figure 2c (left)).¹² The average height of trenches was observed to increase from -10 to $+10$ nm after incubating the mouse IgG, indicating the deposition of mouse IgG in the trenches (Figure 2c (right)).¹³ When the anti-mouse IgG-coated nanotubes were incubated in the buffer solution containing the mouse IgG-patterned substrate for 5 h, the antibody¹ nanotubes were observed to attach to the mouse IgG regions (Figure 2d (left)) after washing the substrates with Nanopure water. The section analysis of this AFM image, Figure 2d (right), also supports the biological recognition-driven nanotube immobilization by increasing the height from $+0$ to $+100$ nm, which is consistent with the diameter of template nanotube. Figure 2e, the magnified AFM image of Figure 2d, shows that the multiple antibody nanotubes in the diameter of 100 nm were attached to the mouse IgG regions. The magnified AFM image of the anti-mouse IgG nanotubes in the height mode (inset in Figure 2e) shows that the antibody nanotubes were aligned along the trench while elongated particles were also observed at the upper side of mouse IgG region. At this point, we are still investigating whether those particles are the aggregations of mouse IgG or the nanotube fragments.

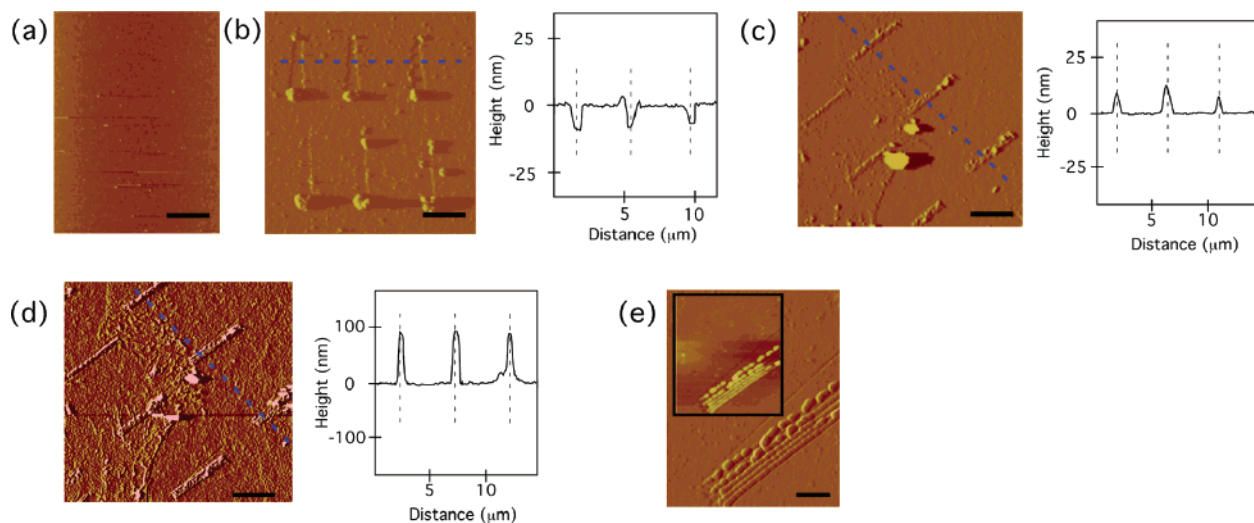


Figure 2. AFM images of (a) alkylthiol SAMs on Au substrate; (b) the array of trenches shaved by the AFM tip (left), the section analysis of (b) along a blue dotted line in the image (right), scale bar = 2 μm ; (c) the array of trenches filled with mouse IgG (left), the section analysis of (c) along a blue dotted line in the image (right), scale bar = 1 μm ; (d) anti-mouse IgG-coated nanotubes immobilized on the mouse IgG-deposited regions (left), the section analysis of (d) along a blue dotted line in the image (right), scale bar = 1 μm ; (e) anti-mouse IgG-coated nanotubes immobilized on the mouse IgG-deposited regions in a higher magnification (inset: in the height mode), scale bar = 300 nm. The positions of trenches in the section analyses (b), (c), and (d), are shown by black dotted lines.

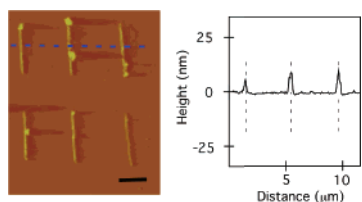


Figure 3. AFM image of the human IgG-deposited regions after the incubation of anti-mouse IgG-coated nanotubes. Scale bar = 2 μm . No anti-mouse IgG nanotubes were observed to attach onto the human IgG regions. Inset: The section analysis along a blue dotted line in the image. The positions of trenches in the section analyses are shown by black dotted lines.

To demonstrate that the assembly of antibody nanotubes is location-specific via biological recognition, the anti-mouse IgG-coated nanotubes were incubated on the substrate patterned with the human IgG instead of the mouse IgG. As shown in Figure 3, no anti-mouse IgG-coated nanotubes attached to the human IgG regions patterned on the alkylthiol SAM/Au substrates via nano-grafting. This control experiment indicates the potential that multiple antibody nanotubes can be addressed onto patterned antigen regions respectively because the biological recognition and complexation of antibody nanotubes with complementary antigen SAMs are very specific, as observed in nature.

In summary, we observed that the biological recognition between the antibody nanotubes and the antigen arrays organized the antibody nanotubes as the ordered arrays. This technique is very useful to fabricate advanced nanometer-scale devices with complex functionalities because multiple building blocks with a variety of protein functions can be addressed to specific locations on substrates respectively in a simple process.

Acknowledgment. This work was supported by the U.S. Department of Energy (DE-FG-02-01ER45935).

Supporting Information Available: Fluorescence micrographs of the Alexa Fluor 546-labeled anti-mouse IgG-coated nanotube and the anti-mouse IgG nanotube coated with the FITC-labeled mouse IgG. This material is available free of charge via the Internet at <http://pubs.acs.org>.

References

- (1) (a) Zhong, Z. H.; Wang, D. L.; Cui, Y.; Bockrath, M. W.; Lieber, C. M. *Science* **2003**, *302*, 1377. (b) Chen, R. J.; Bangsaruntip, S.; Drouvalakis, K. A.; Kam, N. W. S.; Shim, M.; Li, Y. M.; Kim, W.; Utz, P. J.; Dai, H. J. *Proc. Natl. Acad. Sci. U.S.A.* **2003**, *100*, 4984. (c) Fennimore, A. M.; Yuzvinsky, T. D.; Han, W. Q.; Fuhrer, M. S.; Cumings, J.; Zettl, A. *Nature* **2003**, *424*, 408.
- (2) Sumerel, J. L.; Yang, W. J.; Kisailus, D.; Weaver, J. C.; Choi, J. H.; Morse, D. E. *Chem. Mater.* **2003**, *15*, 4804.
- (3) (a) Wang, Q.; Lin, T. W.; Tang, L.; Johnson, J. E.; Finn, M. G. *Angew. Chem., Int. Ed.* **2002**, *41*, 459. (b) Mao, C. B.; Solis, D. J.; Reiss, B. D.; Kottmann, S. T.; Sweeney, R. Y.; Hayhurst, A.; Georgiou, G.; Iverson, B.; Belcher, A. M. *Science* **2004**, *303*, 213. (c) Slocik, J. M.; Moore, J. T.; Wright, D. W. *Nano Lett.* **2002**, *2*, 169. (d) Douglas, T.; Strable, E.; Willits, D.; Aitouchen, A.; Libera, M.; Young, M. *Adv. Mater.* **2002**, *14*, 415. (e) Naik, R. R.; Stringer, S. J.; Agarwal, G.; Jones, S. E.; Stone, M. O. *Nat. Mater.* **2002**, *1*, 169. (f) Sarikaya, M.; Tamerler, C.; Jen, A. K. Y.; Schulten, K. *Nat. Mater.* **2003**, *2*, 577. (g) Sano, K. I.; Shiba, K. J. *Am. Chem. Soc.* **2003**, *125*, 14234. (h) Li, Z.; Chung, S. W.; Nam, J. M.; Ginger, D. S.; Mirkin, C. A. *Angew. Chem., Int. Ed.* **2003**, *42*, 2306.
- (4) Melosh, N. A.; Boukai, A.; Diana, F.; Gerardot, B.; Badolato, A.; Petroff, P. M.; Heath, J. R. *Science* **2003**, *300*, 112.
- (5) Javey, A.; Guo, J.; Wang, Q.; Lundstrom, M.; Dai, H. J. *Nature* **2003**, *424*, 654.
- (6) Rao, S. G.; Huang, L.; Setyawan, W.; Hong, S. H. *Nature* **2003**, *425*, 36.
- (7) Liu, G.-Y.; Xu, S.; Qian, Y. *Acc. Chem. Res.* **2000**, *33*, 457.
- (8) Matsui, H.; Gologan, B. *J. Phys. Chem. B* **2000**, *104*, 3383.
- (9) Kogiso, M.; Ohnishi, S.; Yase, K.; Masuda, M.; Shimizu, T. *Langmuir* **1998**, *14*, 4978.
- (10) (a) Doubberly, G. J.; Pan, S.; Walters, D.; Matsui, H. *J. Phys. Chem. B* **2001**, *105*, 7612. (b) Djalali, R.; Chen, Y.-f.; Matsui, H. *J. Am. Chem. Soc.* **2003**, *125*, 5873. (c) Banerjee, I. A.; Yu, L.; Matsui, H. *Proc. Natl. Acad. Sci. U.S.A.* **2003**, *100*, 14678. (d) Yu, L.; Banerjee, I. A.; Matsui, H. *J. Am. Chem. Soc.* **2003**, *125*, 14837.
- (11) Djalali, R.; Chen, Y.-f.; Matsui, H. *J. Am. Chem. Soc.* **2002**, *124*, 13660.
- (12) Lee, K.-B.; Lim, J.-H.; Mirkin, C. A. *J. Am. Chem. Soc.* **2003**, *125*, 5588.
- (13) Liu, G.-Y.; Amro, N. A. *Proc. Natl. Acad. Sci. U.S.A.* **2002**, *99*, 5165.

JA048617U